

## REVIEW

# Liver-specific agents for contrast-enhanced MRI: role in oncological imaging

Yee Liang Thian<sup>a</sup>, Angela M. Riddell<sup>b</sup>, Dow-Mu Koh<sup>b</sup>

<sup>a</sup>Department of Diagnostic Imaging, National University Hospital Singapore, 5 Lower Kent Ridge Road, Singapore 119074; <sup>b</sup>Department of Diagnostic Radiology, Royal Marsden Hospital Foundation Trust, Downs Road, Sutton, Surrey SM2 5PT, UK

Corresponding address: Dow-Mu Koh, Department of Radiology, Royal Marsden Hospital, Downs Road, Sutton, SM2 5PT, UK.

Email: [dowmukoh@icr.ac.uk](mailto:dowmukoh@icr.ac.uk)

Date accepted for publication 5 November 2013

### Abstract

Liver-specific magnetic resonance (MR) contrast agents are increasingly used in evaluation of the liver. They are effective in detection and morphological characterization of lesions, and can be useful for evaluation of biliary tree anatomy and liver function. The typical appearances and imaging pitfalls of various tumours at MR imaging performed with these agents can be understood by the interplay of pharmacokinetics of these contrast agents and transporter expression of the tumour. This review focuses on the applications of these agents in oncological imaging.

**Keywords:** *Gd-EOB-DTPA; Gd-BOPTA; liver; magnetic resonance imaging; gadoxetic acid; gadobenate.*

### Introduction

Magnetic resonance imaging (MRI) is well established for the imaging assessment of the liver. In addition to conventional MRI performed without contrast or after administration of non-specific extracellular gadolinium chelates, liver-specific contrast agents have been developed to enhance morphological assessment and to provide functional information. The clinical use and application of these agents have undergone a dramatic increase in recent years.

Liver-specific MR contrast agents have been available for over a decade, and are broadly divided into those that are taken up selectively by functionally intact hepatocytes and those that are metabolized by Kupffer cells. Early examples of the former include manganese-based mangafodipir trisodium (Mn-DPDP; Teslascan) and the latter superparamagnetic iron oxide (SPIO) such as ferumoxide (Endorem) and ferucarbotran (Resovist). Despite papers citing their diagnostic utility<sup>[1,2]</sup>, limited clinical use of these agents may have resulted from logistical difficulties of utilizing these in everyday workflow, safety concerns, and lack of commercial success, resulting in their

non-availability<sup>[1–3]</sup>. Ferumoxide, for instance, needed to be infused over 30–60 min while mangafodipir was slowly infused over 10–20 min<sup>[4]</sup>, making them unpopular in busy radiology departments. Moreover, a separate injection of an extracellular gadolinium-based agent might be needed (for ferumoxide) to provide dynamic contrast images, increasing the cost and time of imaging.

By contrast, currently available liver-specific MR contrast media are gadolinium-based compounds, which have overcome many of these earlier shortcomings such as the need for slow intravenous infusion and a protracted imaging time to allow contrast to accumulate in the hepatocytes or Kupffer cells. These agents are increasingly part of the radiologist's toolbox in problem solving for the detection and characterization of hepatic diseases. This review focuses on the two most commonly used hepatobiliary agents commercially available at present: gadobenate dimeglumine (Gd-BOPTA, MultiHance; Bracco Diagnostics) and gadoxetate disodium (Gd-EOB-DTPA, Primovist in Europe and Eovist in the United States; Bayer Healthcare Pharmaceuticals). We discuss their mechanisms of action, MRI protocol, and their diagnostic utility in oncology patients.

## Properties of hepatobiliary contrast agents

Gadobenate dimeglumine and gadoxetic acid are bimodal gadolinium-based chelate contrast agents, which have kinetic properties comprising a distribution phase and elimination phase<sup>[3]</sup>. These phases correspond to the multiphase and hepatocellular phases, which are exploited in hepatobiliary imaging (Fig. 1). An understanding of the pharmacokinetics of these agents is essential to appreciate the relative signal intensity of focal liver lesions to liver parenchyma and to identify confounding factors that can affect the MR signal.

Both agents can be administered as intravascular boluses, which allows for the assessment of vascular structures as well as multiphase contrast alterations within focal lesions. These contrast media initially distribute in the vascular and interstitial compartments, similarly to extracellular contrast agents, during which time hepatic arterial and portal venous phase imaging can be performed. Gadobenate dimeglumine is administered at the manufacturer's recommended dose of 0.1 mmol/kg and has excellent performance during dynamic phase imaging due to its increased signal from an almost 2-fold greater  $T_1$  relaxivity (compared with Gd-DTPA), secondary to its more lipophilic structure and transient interaction with serum albumin<sup>[3]</sup>. Gadoxetic acid similarly has a greater effect on  $T_1$  relaxivity than Gd-DTPA<sup>[5]</sup> and is approved by the US Food and Drug Administration at a dose of 0.025 mmol/kg following

the optimum dose findings in a phase IIB trial<sup>[6]</sup>. At the recommended manufacturer doses, gadobenate dimeglumine has been shown to yield higher maximum enhancement of the hepatic artery, portal vein, and hepatic veins compared with gadoxetic acid<sup>[7,8]</sup>. It has also been shown that although arterial enhancement of gadoxetic acid at this dose provides comparable enhancement of the aorta compared with standard-dose Gd-DTPA, it has lower signal increase of the inferior vena cava, portal vein, and extracellular interstitial enhancement of the liver parenchyma<sup>[9]</sup>. The clinical impact of these differences has not been evaluated.

The hepatic elimination of gadobenate dimeglumine and gadoxetic acid is unique, which is exploited for imaging in the hepatocellular phase. Only 2–4% of gadobenate dimeglumine is cleared via biliary excretion, compared with 50% for gadoxetic acid. The enhancement of the hepatocyte-specific phase plateaus later for gadobenate dimeglumine than for gadoxetic acid (approximately 60–90 min vs 15–25 min)<sup>[3]</sup>. Despite these differences, studies on rhesus monkeys have found that both agents provide comparable maximum enhancement of the liver parenchyma at 1.5 T when equivalent doses of 0.1 mmol/kg are used<sup>[10]</sup>, although another study showed superior signal-to-noise ratio performance during the hepatobiliary phase when a double dose of gadoxetic acid was used at 3 T<sup>[11]</sup>.

More recently, the elimination mechanisms of these agents have been elucidated at the molecular level (Fig. 2). Transport across the hepatocytes is mediated

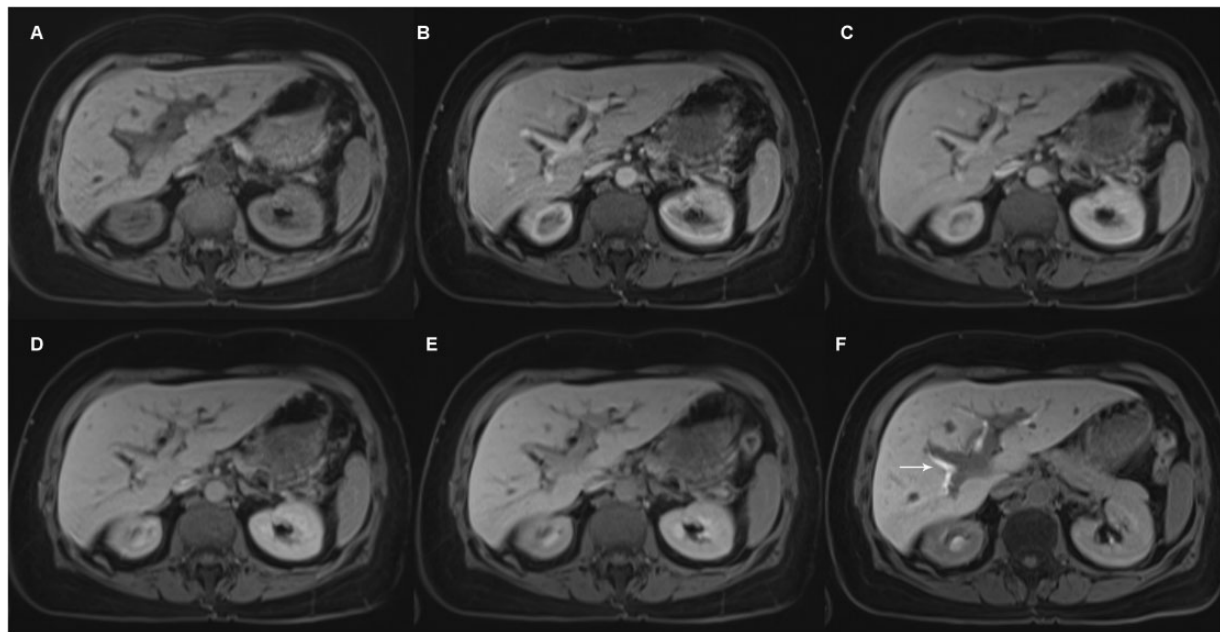


**Figure 1** Axial fat-suppressed  $T_1$ -weighted three-dimensional (3D) gradient recalled echo (GRE) images of a healthy liver with gadoxetic acid administration obtained at (A) precontrast, (B) 30 s, (C) 60 s, (D) 2 min, (E) 5 min, and (F) 20 min. There is progressive enhancement of the liver parenchyma while the portal venous vasculature shows progressive decrease in signal intensity. At 20 min, excreted contrast into the bile ducts (arrow) causes strong enhancement of the biliary tree that is visualized even in the segmental ducts.

by transporting polypeptides located at the sinusoidal and canalicular membranes of hepatocytes<sup>[12]</sup>. Both gadoteric acid and gadobenate dimeglumine agents enter hepatocytes from the sinusoids by active transport through organic anion transporting polypeptides (OATPs)<sup>[13]</sup>, and are excreted into the bile via multidrug resistance protein 2 (MRP2)<sup>[14]</sup>. In addition, efflux back into the sinusoids can occur via bidirectional OATPs or other MRPs<sup>[15]</sup>. The molecular regulation of OATPs and MRPs, and their expression in certain tumour cell types and pathological conditions such as cirrhosis/cholestasis, modifies the imaging appearance in the hepatobiliary phase.

The pharmacological characteristics of gadobenate dimeglumine and gadoteric acid are presented in Table 1.

### MRI protocol optimization

A complete liver imaging protocol would comprise conventional T<sub>1</sub>-weighted and T<sub>2</sub>-weighted imaging, diffusion-weighted imaging, multiphase contrast-enhanced T<sub>1</sub>-weighted imaging, and T<sub>1</sub>-weighted imaging in the

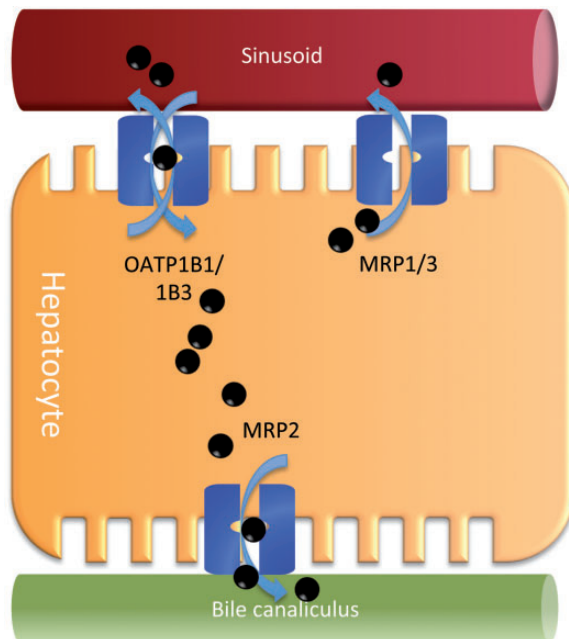


**Figure 2** Schematic diagram of gadoteric acid/gadobenate dimeglumine transport through hepatocytes. Gadoteric acid and gadobenate dimeglumine (represented by black circles) are actively transported from the sinusoids via organic anion transporting polypeptide (OATP) 1B1 and 1B3 into the hepatocytes. They are excreted into the biliary canaliculi via multidrug resistance protein 2 (MRP2) on the canalicular membrane. MRP3 is also involved in efflux of gadoteric acid back to the sinusoids at the basolateral membrane.

hepatocellular phase, which is unique to these agents. Modification of acquisition protocols has been evaluated to optimize image quality and scan time.

With the use of gadoteric acid, a necessary delay occurs between the initial dynamic phase imaging and the hepatocellular phase. To maximize imaging efficiency, this gap provides the opportunity to acquire images that are relatively unaffected by contrast accumulation in the hepatocytes. It has been shown that acquisition of T<sub>2</sub>-weighted and diffusion-weighted images after administration of gadoteric acid has no significant effect on the detection or characterization of focal hepatic lesions and, in fact, improved the lesion-to-liver contrast-to-noise ratio (CNR) on diffusion-weighted images<sup>[16,17]</sup>, likely a result of the shortened liver T<sub>2</sub> relaxation time. Quantification of diffusion-related parameters such as diffusion coefficients and liver shear stiffness values evaluated by magnetic resonance elastography also do not significantly change<sup>[18–20]</sup>.

The image quality of the arterial phase after gadoteric acid injection has been shown to improve, with a slower injection rate of 1 ml/s compared with the standard 2–3 ml/s for non-specific extracellular gadolinium chelates<sup>[9,21,22]</sup>. This contrasts with computed tomography (CT) whereby an increased injection speed and delivery rate of iodine contrast media significantly increased arterial phase enhancement<sup>[23]</sup>. Some proposed reasons for this could be the increased time for gadoteric acid to bind with proteins if the bolus is less compact thus allowing valences to establish, a slower circulation of contrast material leading to more contrast remaining in the arterial vasculature during arterial phase acquisition<sup>[9,24]</sup>, and reduction of truncation artefacts in k-space<sup>[25]</sup>. Interestingly, a recent study found that the bolus administration of gadoteric acid was associated with acute transient dyspnoea, which can result in significant degradation of the arterial phase images in up to 19% of patients<sup>[26]</sup>.

Hepatobiliary phase enhanced MRI is typically performed at 15–20 min for gadoteric acid and 60–120 min for gadobenate dimeglumine. When using gadoteric acid in patients with normal liver function, a delay time of 10 min may be sufficient to characterize and detect focal liver lesions<sup>[27,28]</sup>. However, in cirrhotic livers or severe cholestasis, diminished and delayed enhancement may be seen to arise from reduced functional hepatocellular mass or dysfunction of the transport mechanisms, and a greater delay may be beneficial in these circumstances. However, the relationship between liver function derangements and the degree of liver parenchyma enhancement is not yet accurately established.

Increasing the flip angle of T<sub>1</sub>-weighted images during hepatobiliary phase acquisition can significantly increase lesion detection and improve gadoteric acid depiction of the biliary tree<sup>[29,30]</sup>. Using a higher flip angle (up to 30–35°) increases the signal of the enhanced liver and biliary tracts while decreasing that of unenhanced lesions, thereby providing good CNR to aid lesion

**Table 1** Characteristics of hepatobiliary-specific contrast agents

	Gadoxetic acid	Gadobenate dimeglumine
Trade name	Primovist (Europe) Eovist (USA)	MultiHance
Manufacturer's dosage (mmol/kg body weight)	0.025	0.1
Injection rate	1–2 ml/s	1–2 ml/s
T <sub>1</sub> relaxivity in plasma at 37°C (l/mmol/s)	6.9 (6.5–7.3)	6.3 (6.0–6.6)
Uptake	Organic anion transporters on hepatocytes	Organic anion transporters on hepatocytes
Excretion	50% biliary, 50% renal	3–5% biliary, predominantly renal
Hepatobiliary phase image acquisition	20 min post contrast administration	60–120 min post contrast administration
Side effects	Mild (nausea, flushing, injection-site pain, headache, taste perversion)	Mild (nausea, flushing, injection-site pain, headache, taste perversion)

detection. However, corresponding increases in specific absorption rate should be taken into account, especially at the higher field strength of 3.0 T.

## Diagnostic applications in oncological imaging

In oncological imaging, liver-specific agents are useful for the detection and characterization of lesions, imaging of the biliary tract, and detection of postoperative complications. In the future, these agents may also allow non-invasive assessment of liver function.

### *Hepatocellular carcinoma*

Gadoxetic acid has been shown to improve the detection of hepatocellular carcinoma (HCC) in cirrhotic livers compared with multidetector CT<sup>[31,32]</sup>. Similar to the extracellular contrast agents, HCCs typically show hyperintense T<sub>1</sub> enhancement in the arterial phase, and appear relatively hypointense in the portal venous and delayed phases. During the hepatocellular phase, the avid enhancement of the liver parenchyma provides the background against which lesions lacking functioning normal hepatocytes stand out (Fig. 3). Up to 90% of HCCs are hypointense lesions in the hepatocellular phase because of their lack of functioning hepatocytes<sup>[33]</sup>. However, 10–20% of HCCs remain isointense or even hyperintense during the hepatocellular phase, which has been shown to correlate with the level of expression of OATPs and MRPs in tumour cells<sup>[33,34]</sup>. In one study, it was found that the expression of OATPs and enhancement ratio of HCCs in the hepatocellular phase decreased with poorer tumour differentiation<sup>[35]</sup>, which reflected the known multistep pathogenesis of these tumours.

A common problem in the cirrhotic liver is the early detection of small HCCs and the characterization of small nodules. Small HCCs (<2 cm) are frequently not hypervascular while small hypervascular foci are not always HCC<sup>[36,37]</sup>. Gadoxetic acid has been shown to be useful to detect small HCCs as they appear hypointense during the hepatocellular phase, while hypervascular foci that show isointensity on the hepatocellular phase

are likely pseudolesions<sup>[38]</sup>. In one series, MRI with gadoxetic acid detected up to 90% of small HCCs, compared with 58% using multiphasic multidetector CT<sup>[32,39]</sup>. Gadoxetic acid can also potentially differentiate between early hypovascular HCC and benign hepatocellular nodules such as regenerative or dysplastic nodules, which are usually isointense at hepatocellular phase imaging<sup>[40,41]</sup>.

Hypointense lesions detected in the hepatocellular phase in the cirrhotic population have been found to be associated with malignant potential. In one study, 1-year cumulative risk of progression to conventional HCC of up to 15.6% was observed<sup>[42]</sup>. However, some authors have cautioned that treating these lesions too aggressively in patients who already have HCCs elsewhere may be too severe<sup>[43]</sup>. In the management of the lone hypointense nodule in the hepatocellular phase of imaging, a combination of diffusion-weighted imaging and gadoxetic acid-enhanced imaging has been shown to improve accuracy and sensitivity of diagnosis of HCC compared with either MRI technique alone.<sup>[44]</sup> It is worth re-emphasizing that all other MR sequences and clinical data should be reviewed before deciding on the malignant potential of any target lesion.

There is also emerging data of the usefulness of gadoxetic acid-enhanced MRI as a prognostic biomarker in HCC. One recent study concluded that iso- to hyperintensity on hepatocellular phase images of histologically proven HCCs was correlated with lower histological grade and longer time to tumour recurrence after surgery<sup>[33]</sup>.

There is, unfortunately, a paucity of scientific data directly comparing the diagnostic accuracy of liver-specific gadolinium chelates with non-specific extracellular gadolinium chelates for HCC detection. Park et al.<sup>[45]</sup> found that while gadoxetic acid was more sensitive for HCC detection, analysis by receiver-operator characteristic curves could not demonstrate a significant difference in their diagnostic accuracies.

### *Cholangiocarcinoma*

Cholangiocarcinoma is the second most common primary hepatic malignancy after HCC, with a rising



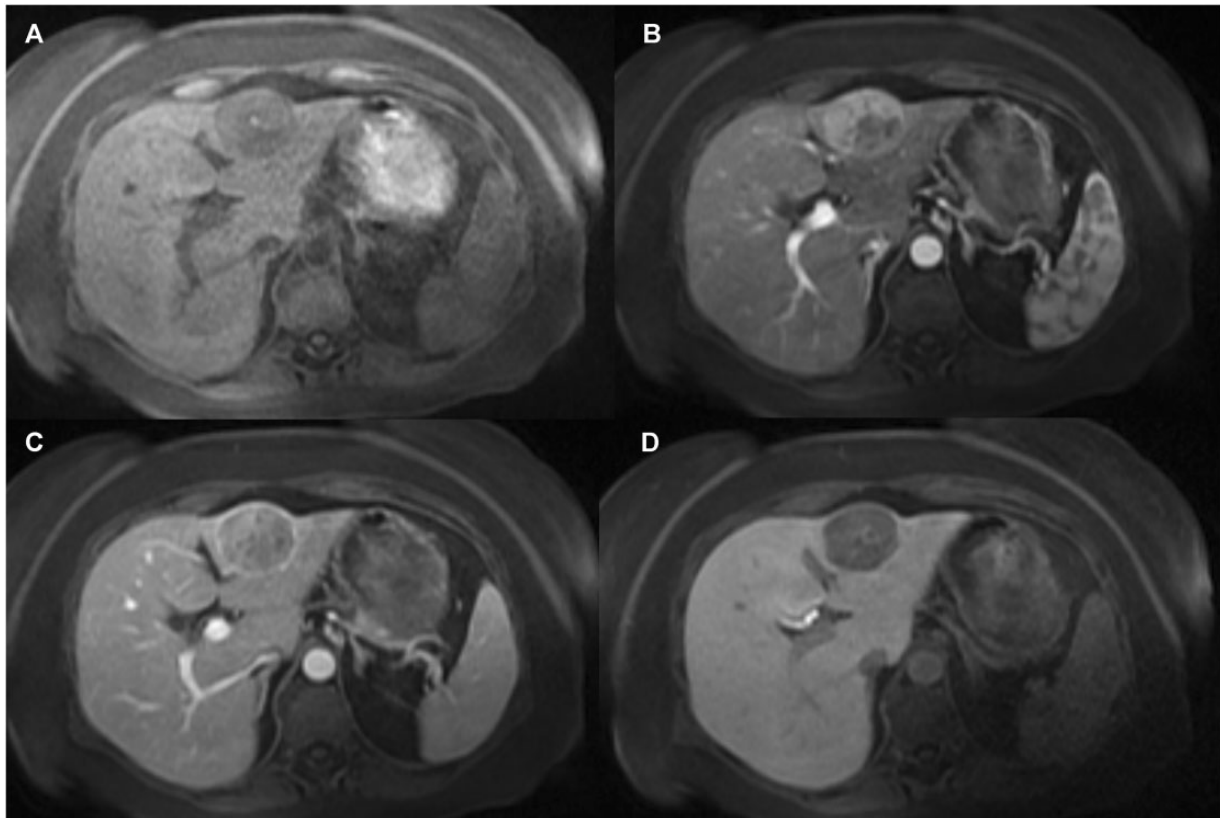


**Figure 3** Axial fat-suppressed T<sub>1</sub>-weighted 3D GRE images of Edmondson grade 3–4 hepatocellular carcinoma in a 72-year-old man. Images obtained during (A) unenhanced phase, (B) arterial phase, and (C) portal venous phase after gadoteric acid administration show characteristic left-lobe hepatocellular carcinoma (HCC) arterial hypervascularity and portal venous washout with a mosaic pattern and pseudocapsule formation. (D) At the 20-min hepatocellular phase, there is strong enhancement of the background liver parenchyma, but no uptake in the HCC.

incidence worldwide<sup>[46]</sup>. With non-specific extracellular gadolinium chelates, they show initial minimal to moderate rim enhancement followed by progressive heterogeneous filling with contrast material<sup>[47]</sup>. Classically the desmoplastic components of cholangiocarcinoma show mild delayed progressive enhancement at 10–20 min after injection, which is observed on both CT and MRI<sup>[48]</sup>.

When imaging mass-forming cholangiocarcinoma with gadoteric acid, there is significant uptake of contrast into normal liver parenchyma during the late venous phase that continues to the hepatobiliary phase. Thus the hyperintensity expected from interstitial accumulation of contrast at the 10–20-min window is reversed because of the relatively greater uptake in surrounding liver parenchyma<sup>[49]</sup>, and most lesions show inhomogeneous hypointensity with intermingled hyperintensity<sup>[50]</sup>. Central hyperintensity (target appearance) has also been observed in the hepatocellular phase, believed to be related to contrast accumulation in the extracellular space of the fibrous stroma in these tumours<sup>[51]</sup>.

The hepatocellular phase often provides the highest conspicuity of cholangiocarcinomas, and there is the

potential of improved detection of additional daughter nodules and intrahepatic metastases<sup>[50]</sup>. In addition, the excretion of contrast into bile ducts may be helpful for the evaluation of ductal cholangiocarcinomas and tumour-related stenosis and duct dilation (Fig. 4). However, in cases of intraductal and periductal infiltrating types of cholangiocarcinoma, there is often associated obstruction of the involved duct with consequent functional impairment of the draining segments. This results in diminished uptake and biliary excretion of hepatobiliary contrast agents, which can limit their diagnostic value.

Therefore, imaging with liver-specific agents is very attractive for preoperative evaluation and therapy planning of cholangiocarcinomas, provided that the liver function is not significantly compromised.

### *Hepatic metastases*

The liver is one of the most common sites for metastatic disease, and secondary liver tumours are far more common than primary hepatic malignancy<sup>[52]</sup>. Accurate detection of hepatic metastases is crucial for treatment planning, especially if curative resection is being

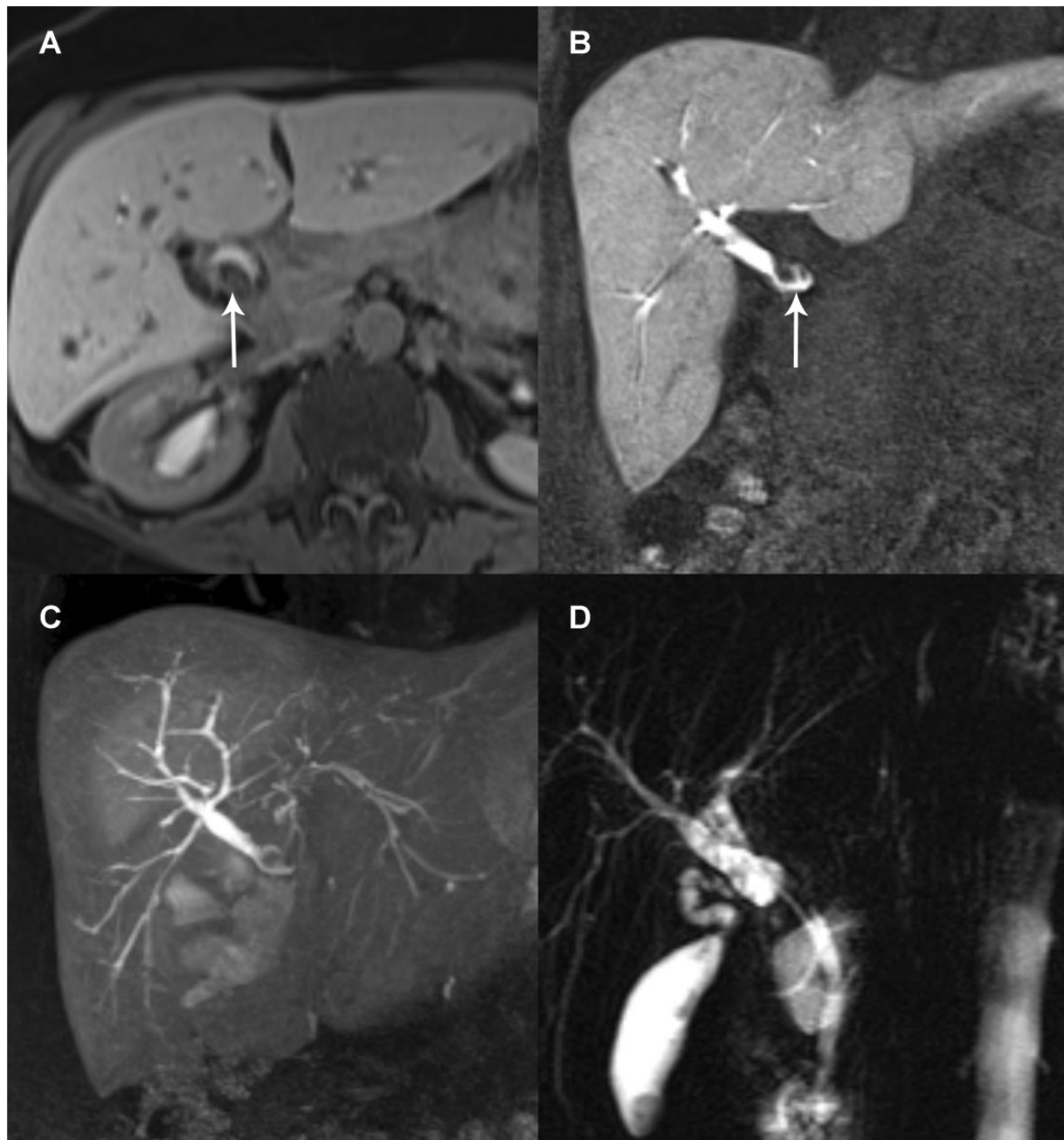


**Figure 4** Ductal type cholangiocarcinoma at the common bile duct in a 58-year-old man. (A, B) Axial and coronal fat-suppressed T<sub>1</sub>-weighted 3D GRE images performed 20 min after gadoteric acid administration show excreted contrast within the biliary radicles adjacent to the hypointense vascular structures of the portal triads. There is a filling defect (arrow) and abrupt truncation of the common bile duct at the site of the obstructing tumour. (C) Maximum-intensity projection of the coronal images produce a T<sub>1</sub>-weighted magnetic resonance cholangiopancreatography (MRCP)-like picture demonstrating the anatomy of the biliary tree. Note that the pancreatic duct and stomach are not hyperintense, unlike on a conventional T<sub>2</sub>-weighted MRCP. (D) T<sub>2</sub>-weighted MRCP performed 2 weeks later after biliary stent insertion.

considered (e.g., in colorectal cancer). Gadoteric acid and gadobenate dimeglumine are useful for detecting liver metastases, with both excellent sensitivity and positive predictive value<sup>[53–56]</sup>. Liver metastases most commonly show a pattern of peripheral ring enhancement on the arterial-dominant phase and incomplete centripetal

progression on the portal venous and delayed phases<sup>[57]</sup>. The presence of a peripheral low-intensity zone or washout on portal venous or equilibrium phases is considered specific for malignancy<sup>[58]</sup>.

As metastatic tumours do not contain functioning hepatocytes or the necessary transporters for the uptake

of gadoxetic acid and gadobenate dimeglumine, they appear hypointense during the hepatocellular phase, resulting in a high contrast between enhancing liver tissue and metastases. Several studies have reported that hepatic metastases frequently show a distinct target appearance on the hepatocellular phase, with a central round hyperintense portion surrounded by a relatively hypointense rim<sup>[59,60]</sup>. This has been attributed to desmoplastic reaction with a large interstitial space in the central portion of the tumour, which retains contrast on delayed imaging. The degree of central paradoxical uptake is typically lower than that of normal liver parenchyma. Delayed interstitial retention of contrast may also account for reports of hepatic metastases in the literature that show unexpected uptake of gadoxetic acid<sup>[61]</sup>.

One of the potential diagnostic pitfalls in using gadoxetic acid-enhanced imaging in the hepatocellular phase to detect liver metastases is that both small metastases and intrahepatic vasculature appear hypointense and can be mistaken for one another. For this reason, the combined reading of these images with diffusion-weighted MRI can help to improve the diagnostic performance of detecting small liver metastases<sup>[62]</sup>.

### *Benign entities: focal nodular hyperplasia, hepatic adenoma, and haemangioma*

Radiologists must be familiar with the appearance of common benign entities in the liver when imaging with hepatocellular agents, as they are frequently incidental findings that can be mistaken for malignancy. Furthermore, using non-specific extracellular gadolinium chelates, it can be difficult to distinguish between focal nodular hyperplasia (FNH) and hepatic adenomas because of overlap in their enhancement features. Using gadoxetic acid or gadobenate dimeglumine can improve the diagnosis of these entities. For liver haemangiomas, the imaging appearances of these (especially if atypical) can mimic malignancy, as they appear hypointense in the hepatocellular phase of contrast-enhanced imaging.

### Focal nodular hyperplasia

FNH is the most common solid benign lesion in the liver<sup>[63]</sup>. It is almost always managed conservatively, and must be differentiated from other solid liver lesions such as hepatic adenomas, HCCs, or metastases, as these lesions require either surveillance or treatment. The classic imaging appearance using non-specific extracellular gadolinium chelates of a well-circumscribed, intensely arterially enhancing lesion with a central fibrous scar that is hyperintense on T<sub>2</sub>-weighted images and shows delayed enhancement, is probably seen in fewer than 50% of FNH lesions<sup>[64,65]</sup>. These features are even less common in small lesions. Imaging with hepatocellular

agents increases confidence in making the radiologic diagnosis, thus avoiding invasive biopsy.

As FNHs are essentially hyperplastic hepatocellular cells with preserved transporter function containing malformed bile ducts, the majority appear hyperintense on hepatocellular phase imaging. Other imaging patterns observed are inhomogeneous hyperintensity, isointense pattern, and hypointensity with a hyperintense ring<sup>[66]</sup>. A small percentage (4–10%) of FNHs are completely hypointense during the hepatobiliary phase<sup>[66–68]</sup>, which may be associated with severe ductular metaplasia and diminished functionality of the bile canaliculi<sup>[66]</sup>. The central scar, if present, appears hypointense at hepatocellular phase imaging (Fig. 5).

### Hepatocellular adenoma

Hepatocellular adenomas (HCAs) are benign hepatic neoplasms of hepatocellular origin, but must be differentiated from FNH because of their risks of haemorrhage and malignant transformation to HCC<sup>[69]</sup>. A new classification of hepatic adenomas by the Bordeaux group based on genotype/phenotype has potential to refine the management of HCAs, as it provides more accurate prediction of the risk of haemorrhage and malignant transformation<sup>[70]</sup>. MRI findings of a vaguely demarcated scar and poorly delineated high-signal-intensity areas on T<sub>2</sub>-weighted images seem to correlate with  $\beta$ -catenin positivity, which carries a higher risk of malignancy<sup>[71]</sup>.

Distinguishing between FNH and adenoma on imaging was problematic before the advent of hepatobiliary agents, due to overlap in their imaging features. Intratumoral haemorrhage or fat, which is seen as hyperintensity on T<sub>1</sub>-weighted images, is only variably demonstrated in HCAs. Similar to FNHs, they are hypervascular during the late arterial phase, although the mean enhancement ratio of HCAs has been shown to be significantly lower than that of FNHs<sup>[72]</sup>. On portal venous and equilibrium phases they can be hypointense, isointense, or hyperintense to the liver<sup>[72,73]</sup>.

In contrast to FNHs, the majority of hepatic adenomas (90–100%) are hypointense<sup>[68,73]</sup> on the hepatocellular phase of either gadoxetic acid- or gadobenate dimeglumine-enhanced MRI. This is likely related to the down-regulation of OATPs<sup>[74]</sup> or the lack of biliary canaliculi in HCAs. The addition of the hepatobiliary phase increases sensitivity and accuracy for the diagnosis of hepatic adenomas compared with conventional morphological and dynamic sequences alone<sup>[75,76]</sup>.

An important consideration is that hepatic adenomas may have an appearance similar to that of HCCs on imaging with hepatocellular contrast agents; that is, they show a hypervascular arterial phase, washout in the portal venous or equilibrium phase, and appear hypointense in the hepatocellular phase. Therefore the patient demographics and clinical risk factors must be borne in mind when interpreting the scan. HCCs usually arise against a background of cirrhosis or chronic

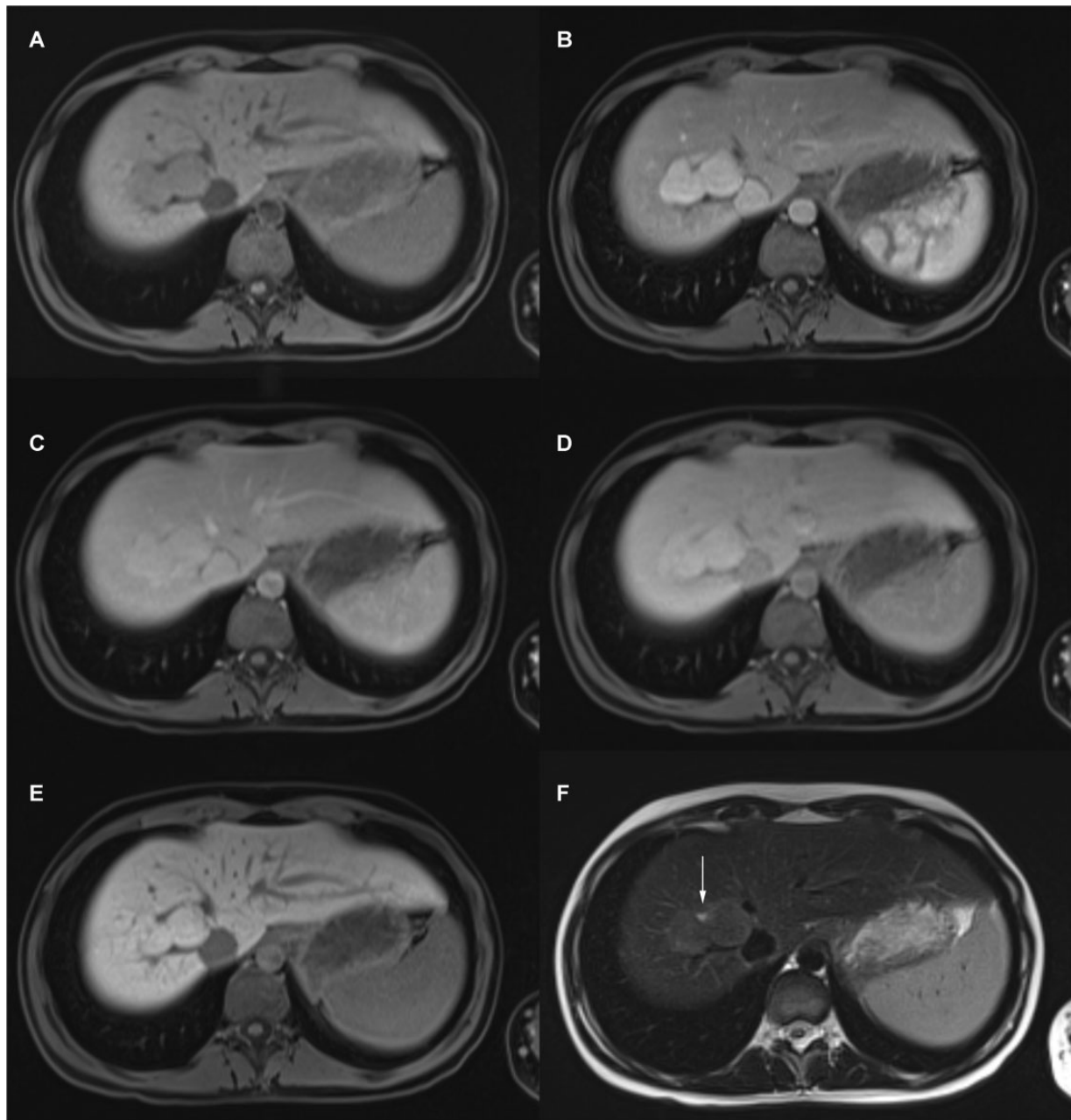


**Figure 5** Axial fat-suppressed T<sub>1</sub>-weighted 3D GRE images of focal nodular hyperplasia (FNH). Images obtained during (A) unenhanced phase, (B) late arterial phase, and (C) portal venous phase with gadoxetic acid show avid homogeneous arterial enhancement persisting on the portal venous phase. (D) At 3 min after contrast injection, the liver shows increasing parenchymal enhancement whereas the vessels are isointense to hypointense. (E) At the 20-min hepatocellular phase, there is strong enhancement of the background liver but equivalently strong gadoxetic acid uptake in the FNH, which thus appears isointense to the liver. As contrast is no longer circulating within the intravascular compartment, the vessels appear as branching hypointense reticular structures. (F) Axial T<sub>2</sub>-weighted image showing the hyperintense scar (arrow) and almost isointense appearance of FNH.

hepatitis, whereas hepatic adenomas are more frequent in young women of childbearing age.

### Haemangioma

Like all other lesions that do not contain functional hepatocytes, haemangiomas are hypointense at hepatocellular

phase imaging. The dynamic phases and T<sub>2</sub>-weighted sequences are thus crucial for differentiating them from more sinister lesions such as metastases.

The dynamic enhancement patterns of hepatic haemangiomas differ significantly between gadobenate dimeglumine and gadoxetic acid, because of differences in



their pharmacokinetics<sup>[77]</sup>. When imaging is performed with gadoxetic acid, haemangiomas may appear hypointense relative to liver parenchyma during the equilibrium and delayed phases, as there will be substantial liver parenchymal uptake from as early as 3–5 min after injection, producing the so-called pseudo-washout sign, which can mimic a hypervascular tumour<sup>[78]</sup>. Thus, the expected prolonged enhancement due to filling in of haemangiomas is less readily observable because of intense liver parenchymal enhancement<sup>[79]</sup> (Fig. 6). This conundrum is less prevalent when gadobenate dimeglumine is used as the contrast agent<sup>[80]</sup>, as there is greater temporal separation between the distribution phase, wherein the dynamic enhancement pattern of the haemangioma is observed, and the biliary elimination phase, when hepatocellular enhancement predominates.

If the multiphasic imaging findings of haemangiomas are atypical with a hepatocellular contrast agent such as gadoxetic acid, the T<sub>2</sub>-weighted sequences are usually sufficiently discriminatory<sup>[81]</sup>. Some authors have suggested T<sub>1</sub> quantitative mapping or additional dynamic imaging with a non-specific extracellular contrast agent<sup>[79]</sup>.

### *Biliary tract imaging for preoperative and postoperative assessment*

Hepatobiliary-specific agents are excreted into the biliary tree, producing T<sub>1</sub> shortening of bile, and thus can be used for contrast-enhanced T<sub>1</sub>-weighted MR cholangiography<sup>[82]</sup>. In combination with conventional T<sub>2</sub>-weighted MR cholangiopancreatography (MRCP), biliary anatomic variants and the relationship between hepatic tumours and the intrahepatic biliary ducts can be assessed, providing the surgeon with a preoperative road map. Gadoxetic acid MR cholangiography has also been shown to be highly reliable for detecting biliary leaks after hepatobiliary surgery<sup>[83]</sup>. Visualization of excreted contrast outside of the bile ducts indicates a bile leak.

T<sub>2</sub>-weighted MRCP should be performed before contrast injection because the presence of excreted concentrated gadolinium in the biliary tree causes T<sub>2</sub> shortening, which may confound the signal on T<sub>2</sub>-weighted MRCP sequences. The excretion of hepatobiliary-specific agents is impaired in patients with obstructive jaundice or focal cholestasis. This may result in non-excretion or delayed

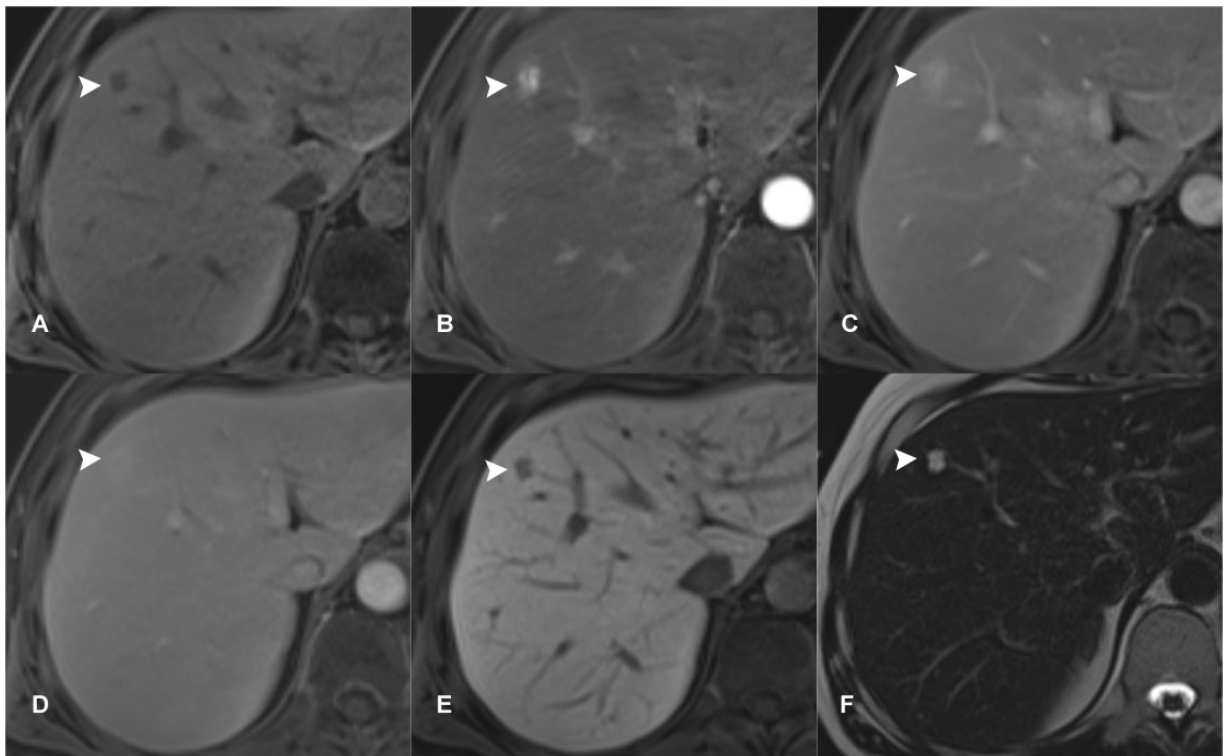


**Figure 6** Axial fat-suppressed T<sub>1</sub>-weighted 3D GRE images of a small haemangioma. Images obtained during (A) unenhanced phase, (B) arterial phase, and (C) portal venous phase after gadoxetic acid administration show the arterially enhancing lesion (arrowhead) with persistent hyperintensity on the portal venous phase. However, at 90 s (D), increasing uptake of gadoxetic acid in the liver results in diminished relative hyperintensity of the blood pool within the haemangioma. (E) At the 20-min hepatocellular phase, the haemangioma appears as a hypointense lesion (arrowhead) against the enhanced liver background. (F) Axial T<sub>2</sub>-weighted image showing the classical light-bulb sign of the haemangioma.

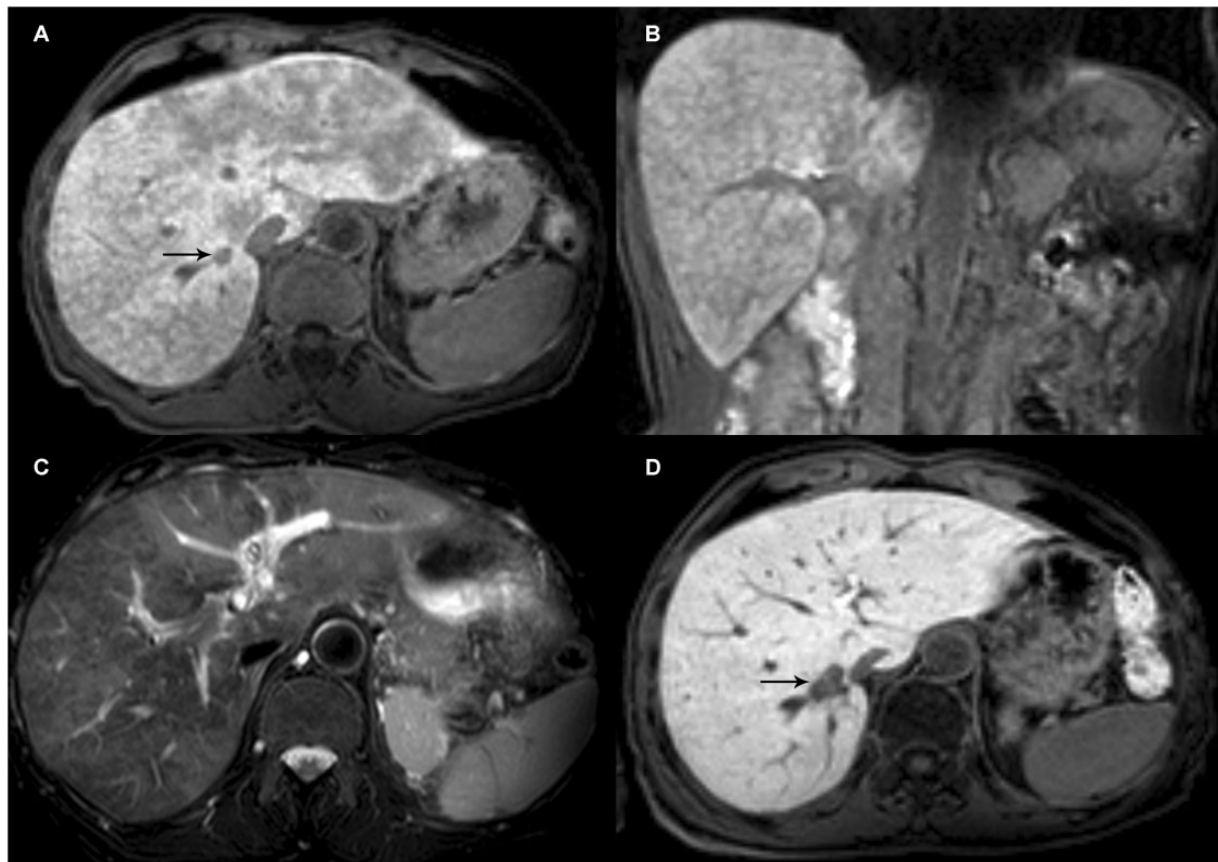


**Figure 7** Sinusoidal obstruction syndrome in a 68-year-old man with colorectal metastases on oxaliplatin. (A, B) Axial and coronal fat-suppressed T<sub>1</sub>-weighted 3D GRE images obtained 20 min after gadoxetic acid administration show characteristic reticular hypointensities in non-tumoural portions of the liver. A small focal hypointense lesion (arrow) adjacent to the right hepatic vein is a metastatic deposit. (C) Axial fat-suppressed T<sub>2</sub>-weighted image shows patchy areas of hyperintensity that may be related to oedema. (D) Oxaliplatin was discontinued, and the follow-up scan performed with gadoxetic acid 5 months later shows resolution of the findings. Unfortunately, there is progression of hepatic metastases (arrow).

excretion of the agent in the entire liver or focal segments of the liver, limiting evaluation of the bile ducts in the involved region on T<sub>1</sub>-weighted MR cholangiography. Although contrast-enhanced MR cholangiography is a useful adjunct, it cannot replace T<sub>2</sub>-weighted MRCP.

#### *Assessment of liver function and toxicity*

Recently there has been increased interest in the use of gadoxetic acid for quantitative evaluation of liver function, and several studies have shown good correlation between the relative signal intensity of the liver at the hepatobiliary phase and the liver function and stage of fibrosis<sup>[84–86]</sup>. Preoperative prediction of liver function is important to provide a gauge of the hepatic functional reserve, which determines the maximum extent of hepatectomy possible to avoid postoperative liver failure<sup>[87]</sup>. A proof-of-concept study investigating the role of gadoxetic acid in preoperative assessment found that lower relative enhancement of gadoxetic acid on hepatobiliary phase images before major liver resection was associated with

increased risk of post-hepatectomy liver failure<sup>[88]</sup>. Further studies are still necessary to confirm the clinical utility of gadoxetic acid-enhanced MRI in this context.

Sinusoidal obstruction syndrome (SOS) is an adverse side effect of systemic chemotherapy for metastatic colorectal cancer, characterized histologically by sinusoidal obstruction, perisinusoidal fibrosis, and veno-occlusion of the non-tumoural liver<sup>[89]</sup>. Although SOS is usually asymptomatic, it may have implications on the timing of hepatic resection and planning of further chemotherapy<sup>[90,91]</sup>. On the hepatocellular phase images of gadoxetic acid-enhanced MRI, reticular hypointensity of non-tumoural liver is indicative of SOS, with high specificity<sup>[91]</sup> (Fig. 7).

## Conclusion

An understanding of the interplay of pharmacokinetics of hepatobiliary contrast agents, histological characteristics of the underlying disease, and the effect of background

liver function aids in the interpretation of MRI scans performed using the hepatocyte-selective gadolinium-based contrast media. The use of these liver-specific MRI contrast agents to improve patient management is expected to grow in oncological imaging.

### Conflict of interest

The authors declare that they have no conflicts of interest.

### References

- [1] Oudkerk M, Torres CG, Song B, et al. Characterization of liver lesions with mangafodipir trisodium-enhanced MR imaging: multicenter study comparing MR and dual-phase spiral CT. *Radiology* 2002; 223: 517–524.
- [2] Koh KC, Kim HJ, Choe WH, et al. The clinical usefulness of SPIO-MRI in detection and staging of hepatocellular carcinoma. *Taehan Kan Hakhoe Chi* 2003; 9: 17–24.
- [3] Reimer P, Schneider G, Schima W. Hepatobiliary contrast agents for contrast-enhanced MRI of the liver: properties, clinical development and applications. *Eur Radiol* 2004; 14: 559–578.
- [4] Gandhi SN, Brown MA, Wong JG, Aguirre DA, Sirlin CB. MR contrast agents for liver imaging: what, when, how. *Radiographics* 2006; 26: 1621–1636.
- [5] Rohrer M, Bauer H, Mintorovitch J, Requardt M, Weinmann H-J. Comparison of magnetic properties of MRI contrast media solutions at different magnetic field strengths. *Invest Radiol* 2005; 40: 715–724.
- [6] Reimer P, Rummeny EJ, Shamsi K, et al. Phase II clinical evaluation of Gd-EOB-DTPA: dose, safety aspects and pulse sequence. *Radiology* 1996; 199: 177–183.
- [7] Brismar TB, Dahlstrom N, Edsberg N, Persson A, Smedby O, Albiin N. Liver vessel enhancement by Gd-BOPTA and Gd-EOB-DTPA: a comparison in healthy volunteers. *Acta Radiol* 2009; 50: 709–715.
- [8] Tamada T, Ito K, Sone T, et al. Dynamic contrast-enhanced magnetic resonance imaging of abdominal solid organ and major vessel: comparison of enhancement effect between Gd-EOB-DTPA and Gd-DTPA. *J Magn Reson Imaging* 2009; 29: 636–640.
- [9] Zech CJ, Vos B, Nordell A, et al. Vascular enhancement in early dynamic liver MR imaging in an animal model: comparison of two injection regimen and two different doses Gd-EOB-DTPA (gadoteric acid) with standard Gd-DTPA. *Invest Radiol* 2009; 44: 305–310.
- [10] Runge VM. A comparison of two MR hepatobiliary gadolinium chelates: Gd-BOPTA and Gd-EOB-DTPA. *J Comput Assist Tomogr* 1998; 22: 643–650.
- [11] Frydrychowicz A, Nagle SK, D'Souza SL, Vigen KK, Reeder SB. Optimized high-resolution contrast-enhanced hepatobiliary imaging at 3 tesla: a cross-over comparison of gadobenate dimeglumine and gadoteric acid. *J Magn Reson Imaging* 2011; 34: 585–594.
- [12] Planchamp C, Hadengue A, Stieger B, et al. Function of both sinusoidal and canalicular transporters controls the concentration of organic anions within hepatocytes. *Mol Pharmacol* 2007; 71: 1089–1097.
- [13] Leonhardt M, Keiser M, Oswald S, et al. Hepatic uptake of the magnetic resonance imaging contrast agent Gd-EOB-DTPA: role of human organic anion transporters. *Drug Metab Dispos* 2010; 38: 1024–1108.
- [14] Tsuboyama T, Onishi H, Kim T, et al. Hepatocellular carcinoma: hepatocyte-selective enhancement at gadoteric acid-enhanced MR imaging—correlation with expression of sinusoidal and canalicular transporters and bile accumulation. *Radiology* 2010; 255: 824–833.
- [15] Millet P, Moulin M, Stieger B, Daali Y, Pastor CM. How organic anions accumulate in hepatocytes lacking Mrp2: evidence in rat liver. *J Pharmacol Exp Ther* 2011; 336: 624–632.
- [16] Choi SA, Lee SS, Jung I-H, Kim HA, Byun JH, Lee MG. The effect of gadoteric acid enhancement on lesion detection and characterisation using T2 weighted imaging and diffusion weighted imaging of the liver. *Br J Radiol* 2012; 85: 29–36.
- [17] Ahn SJ, Kim M-J, Hong H-S, Kim KA, Song H-T. Distinguishing hemangiomas from malignant solid hepatic lesions: a comparison of heavily T2-weighted images obtained before and after administration of gadoteric acid. *J Magn Reson Imaging* 2011; 34: 310–317.
- [18] Colagrande S, Mazzoni LN, Mazzoni E, Pradella S. Effects of gadoteric acid on quantitative diffusion-weighted imaging of the liver. *J Magn Reson Imaging* 2012; 36: 881–889.
- [19] Motosugi U, Ichikawa T, Sou H, et al. Effects of gadoteric acid on liver elasticity measurement by using magnetic resonance elastography. *Magn Reson Imaging* 2012; 30: 128–132.
- [20] Muhi A, Ichikawa T, Motosugi U, Sou H, Sano K, Araki T. Diffusion- and T2-weighted MR imaging of the liver: effect of intravenous administration of gadoteric acid disodium. *Magn Reson Med Sci* 2012; 11: 185–191.
- [21] Tamada T, Ito K, Yoshida K, et al. Comparison of three different injection methods for arterial phase of Gd-EOB-DTPA enhanced MR imaging of the liver. *Eur J Radiol* 2011; 80: e284–e288.
- [22] Tanimoto AA, Higuchi NN, Ueno AA. Reduction of ringing artifacts in the arterial phase of gadoteric acid-enhanced dynamic MR imaging. *Magn Reson Med Sci* 2011; 11: 91–97.
- [23] Mitsuzaki K, Yamashita Y, Ogata I, Nishiharu T, Urata J, Takahashi M. Multiple-phase helical CT of the liver for detecting small hepatomas in patients with liver cirrhosis: contrast-injection protocol and optimal timing. *AJR Am J Roentgenol* 1996; 167: 753–757.
- [24] Chung S-H, Kim M-J, Choi JY, Hong H-S. Comparison of two different injection rates of gadoteric acid for arterial phase MRI of the liver. *J Magn Reson Imaging* 2010; 31: 365–372.
- [25] Tanimoto A, Higuchi N, Ueno A. Reduction of ringing artifacts in the arterial phase of gadoteric acid-enhanced dynamic MR imaging. *Magn Reson Med Sci* 2012; 11: 91–97.
- [26] Davenport MS, Viglianti BL, Al-Hawary MM, et al. Comparison of acute transient dyspnea after intravenous administration of gadoterate disodium and gadobenate dimeglumine: effect on arterial phase image quality. *Radiology* 2013; 266: 452–461.
- [27] van Kessel CS, Veldhuis WB, van den Bosch MAAJ, van Leeuwen MS. MR liver imaging with Gd-EOB-DTPA: a delay time of 10 minutes is sufficient for lesion characterisation. *Eur Radiol* 2012; 22: 2153–2160.
- [28] Jeong HT, Kim M-J, Park M-S, et al. Detection of liver metastases using gadoteric acid-enhanced dynamic 10- and 20-minute delayed phase MR imaging. *J Magn Reson Imaging* 2012; 35: 635–643.
- [29] Kim S, Mussi TC, Lee LJ, Mausner EV, Cho KC, Rosenkrantz AB. Effect of flip angle for optimization of image quality of gadoterate disodium-enhanced biliary imaging at 1.5 T. *AJR Am J Roentgenol* 2013; 200: 90–96. doi: 10.2214/AJR.12.8722.
- [30] Haradome H, Grazioli L, Al manea K, et al. Gadoteric acid disodium-enhanced hepatocyte phase MRI: can increasing the flip angle improve focal liver lesion detection? *J Magn Reson Imaging* 2012; 35: 132–139.
- [31] Kim SH, Kim SH, Lee J, et al. Gadoteric acid-enhanced MRI versus triple-phase MDCT for the preoperative detection of hepatocellular carcinoma. *AJR Am J Roentgenol* 2009; 192: 1675–1681.
- [32] Hwang J, Kim SH, Lee MW, Lee JY. Small ( $\leq 2$  cm) hepatocellular carcinoma in patients with chronic liver disease: comparison of gadoteric acid-enhanced 3.0 T MRI and multiphase 64-multirow detector CT. *Br J Radiol* 2012; 85: e314–e322.



- [33] Choi JW, Lee JM, Kim SJ, et al. Hepatocellular carcinoma: imaging patterns on gadoxetic acid-enhanced MR images and their value as an imaging biomarker. *Radiology* 2013; 267: 776–786.
- [34] Kitao A, Zen Y, Matsui O, et al. Hepatocellular carcinoma: signal intensity at gadoxetic acid-enhanced MR imaging—correlation with molecular transporters and histopathologic features. *Radiology* 2010; 256: 817–826.
- [35] Kitao A, Matsui O, Yoneda N, et al. The uptake transporter OATP8 expression decreases during multistep hepatocarcinogenesis: correlation with gadoxetic acid enhanced MR imaging. *Eur Radiol* 2011; 21: 2056–2066.
- [36] Efremidis SC, Hytioglou P, Matsui O. Enhancement patterns and signal-intensity characteristics of small hepatocellular carcinoma in cirrhosis: pathologic basis and diagnostic challenges. *Eur Radiol* 2007; 17: 2969–2982.
- [37] Shimizu A, Ito K, Koike S, Fujita T, Shimizu K, Matsunaga N. Cirrhosis or chronic hepatitis: evaluation of small (< or =2-cm) early-enhancing hepatic lesions with serial contrast-enhanced dynamic MR imaging. *Radiology* 2003; 226: 550–555.
- [38] Sun HY, Lee JM, Shin CI, et al. Gadoxetic acid-enhanced magnetic resonance imaging for differentiating small hepatocellular carcinomas (< or =2 cm in diameter) from arterial enhancing pseudolesions: special emphasis on hepatobiliary phase imaging. *Invest Radiol* 2010; 45: 96–103.
- [39] Haradome H, Grazioli L, Tinti R, et al. Additional value of gadoxetic acid-DTPA-enhanced hepatobiliary phase MR imaging in the diagnosis of early-stage hepatocellular carcinoma: comparison with dynamic triple-phase multidetector CT imaging. *J Magn Reson Imaging* 2011; 34: 69–78.
- [40] Rhee H, Kim MJ, Park MS, Kim KA. Differentiation of early hepatocellular carcinoma from benign hepatocellular nodules on gadoxetic acid-enhanced MRI. *Br J Radiol* 2012; 85: e837–e844.
- [41] Sano K, Ichikawa T, Motosugi U, et al. Imaging study of early hepatocellular carcinoma: usefulness of gadoxetic acid-enhanced MR imaging. *Radiology* 2011; 261: 834–844.
- [42] Motosugi U, Ichikawa T, Sano K, et al. Outcome of hypovascular hepatic nodules revealing no gadoxetic acid uptake in patients with chronic liver disease. *J Magn Reson Imaging* 2011; 34: 88–94.
- [43] Akai H, Matsuda I, Kiryu S, et al. Fate of hypointense lesions on Gd-EOB-DTPA-enhanced magnetic resonance imaging. *Eur J Radiol* 2012; 81: 2973–2977.
- [44] Park MJ, Kim YK, Lee MW, et al. Small hepatocellular carcinomas: improved sensitivity by combining gadoxetic acid-enhanced and diffusion-weighted MR imaging patterns. *Radiology* 2012; 264: 761–770.
- [45] Park G, Kim YK, Kim CS, Yu HC, Hwang SB. Diagnostic efficacy of gadoxetic acid-enhanced MRI in the detection of hepatocellular carcinomas: comparison with gadopentetate dimeglumine. *Br J Radiol* 2010; 83: 1010–1016.
- [46] Khan SA, Thomas HC, Davidson BR, Taylor-Robinson SD. Cholangiocarcinoma. *Lancet* 2005; 366: 1303–1314.
- [47] Maetani Y, Itoh K, Watanabe C, et al. MR imaging of intrahepatic cholangiocarcinoma with pathologic correlation. *AJR Am J Roentgenol* 2001; 176: 1499–1507.
- [48] Lacomis JM, Baron RL, Oliver JH, Nalesnik MA, Federle MP. Cholangiocarcinoma: delayed CT contrast enhancement patterns. *Radiology* 1997; 203: 98–104.
- [49] Péporté ARJ, Sommer WH, Nikolaou K, Reiser MF, Zech CJ. Imaging features of intrahepatic cholangiocarcinoma in Gd-EOB-DTPA-enhanced MRI. *Eur J Radiol* 2013; 82: e101–e106.
- [50] Kang Y, Lee JM, Kim SH, Han JK, Choi BI. Intrahepatic mass-forming cholangiocarcinoma: enhancement patterns on gadoxetic acid-enhanced MR images. *Radiology* 2012; 264: 751–760.
- [51] Kim SH, Lee CH, Kim BH, et al. Typical and atypical imaging findings of intrahepatic cholangiocarcinoma using gadolinium ethoxybenzyl diethylenetriamine pentaacetic acid-enhanced magnetic resonance imaging. *J Comput Assist Tomogr* 2012; 36: 704–709.
- [52] Bosch FX, Ribes J, Díaz M, Cléries R. Primary liver cancer: worldwide incidence and trends. *Gastroenterology* 2004; 127(Suppl 1): S5–S16.
- [53] Chan VO, Das JP, Gerstenmaier JF, et al. Diagnostic performance of MDCT, PET/CT and gadoxetic acid (Primovist®)-enhanced MRI in patients with colorectal liver metastases being considered for hepatic resection: initial experience in a single centre. *Ir J Med Sci* 2012; 181: 499–509.
- [54] Berger-Kulemann V, Schima W, Baroud S, et al. Gadoxetic acid-enhanced 3.0 T MR imaging versus multidetector-row CT in the detection of colorectal metastases in fatty liver using intraoperative ultrasound and histopathology as a standard of reference. *Eur J Surg Oncol* 2012; 38: 670–676.
- [55] Kim YK, Park G, Kim CS, Yu HC, Han YM. Diagnostic efficacy of gadoxetic acid-enhanced MRI for the detection and characterisation of liver metastases: comparison with multidetector-row CT. *Br J Radiol* 2012; 85: 539–547.
- [56] Runge VM, Lee C, Williams NM. Detectability of small liver metastases with gadolinium BOPTA. *Invest Radiol* 1997; 32: 557–565.
- [57] Danet I-M, Semelka RC, Leonardou P, et al. Spectrum of MRI appearances of untreated metastases of the liver. *AJR Am J Roentgenol* 2003; 181: 809–817.
- [58] Mahfouz AE, Hamm B, Wolf KJ. Peripheral washout: a sign of malignancy on dynamic gadolinium-enhanced MR images of focal liver lesions. *Radiology* 1994; 190: 49–52.
- [59] Ha S, Lee CH, Kim BH, et al. Paradoxical uptake of Gd-EOB-DTPA on the hepatobiliary phase in the evaluation of hepatic metastasis from breast cancer: is the “target sign” a common finding? *Magn Reson Imaging* 2012; 30: 1083–1090.
- [60] Kim YK, Lee JM, Kim CS. Gadobenate dimeglumine-enhanced liver MR imaging: value of dynamic and delayed imaging for the characterization and detection of focal liver lesions. *Eur Radiol* 2004; 14: 5–13.
- [61] Song WS, Schwoppe RB, Taylor KA, Lisanti CJ. Unexpected uptake of gadoxetic acid in a hepatic metastasis from T-cell lymphoma. *Cancer Imaging* 2012; 12: 122–125.
- [62] Koh DM, Collins DJ, Wallace T, Chau I, Riddell AM. Combining diffusion-weighted MRI with Gd-EOB-DTPA-enhanced MRI improves the detection of colorectal liver metastases. *Br J Radiol* 2012; 85: 980–989.
- [63] Buell JF, Tranchart H, Cannon R, Dagher I. Management of benign hepatic tumors. *Surg Clin North Am* 2010; 90: 719–735.
- [64] Bioulac-Sage P, Balabaud C, Wanless IR. Diagnosis of focal nodular hyperplasia: not so easy. *Am J Surg Pathol* 2001; 25: 1322–1325.
- [65] Nguyen BN, Fléjou JF, Terris B, Belghiti J, Degott C. Focal nodular hyperplasia of the liver: a comprehensive pathologic study of 305 lesions and recognition of new histologic forms. *Am J Surg Pathol* 1999; 23: 1441–1454.
- [66] van Kessel CS, de Boer E, Kate FJWT, Brosens LAA, Veldhuis WB, van Leeuwen MS. Focal nodular hyperplasia: hepatobiliary enhancement patterns on gadoxetic-acid contrast-enhanced MRI. *Abdom Imaging* 2012; 38: 490–501.
- [67] Zech CJ, Grazioli L, Breuer J, Reiser MF, Schoenberg SO. Diagnostic performance and description of morphological features of focal nodular hyperplasia in Gd-EOB-DTPA-enhanced liver magnetic resonance imaging: results of a multicenter trial. *Invest Radiol* 2008; 43: 504–511.
- [68] Grazioli L, Morana G, Kirchin MA, Schneider G. Accurate differentiation of focal nodular hyperplasia from hepatic adenoma at gadobenate dimeglumine-enhanced MR imaging: prospective study. *Radiology* 2005; 236: 166–177.
- [69] Stoot JHMB, Coelen RJS, De Jong MC, Dejong CHC. Malignant transformation of hepatocellular adenomas into hepatocellular carcinomas: a systematic review including more than 1600 adenoma cases. *HPB (Oxford)* 2010; 12: 509–522.



- [70] Bioulac-Sage P, Balabaud C, Zucman-Rossi J. Subtype classification of hepatocellular adenoma. *Dig Surg* 2010; 27: 39–45.
- [71] van Aalten SM, Thomeer MGJ, Terkivatan T, et al. Hepatocellular adenomas: correlation of MR imaging findings with pathologic subtype classification. *Radiology* 2011; 261: 172–181.
- [72] Grazioli L, Bondioni MP, Haradome H, et al. Hepatocellular adenoma and focal nodular hyperplasia: value of gadoxetic acid-enhanced MR imaging in differential diagnosis. *Radiology* 2012; 262: 520–529.
- [73] Denecke T, Steffen IG, Agarwal S, et al. Appearance of hepatocellular adenomas on gadoxetic acid-enhanced MRI. *Eur Radiol* 2012; 22: 1769–1775.
- [74] Vander Borgh S, Libbrecht L, Blokzijl H, et al. Diagnostic and pathogenetic implications of the expression of hepatic transporters in focal lesions occurring in normal liver. *J Pathol* 2005; 207: 471–482.
- [75] Bieze M, van den Esschert JW, Nio CY, et al. Diagnostic accuracy of MRI in differentiating hepatocellular adenoma from focal nodular hyperplasia: prospective study of the additional value of gadoxetate disodium. *AJR Am J Roentgenol* 2012; 199: 26–34.
- [76] Purysko AS, Remer EM, Coppa CP, Obuchowski NA, Schneider E, Veniero JC. Characteristics and distinguishing features of hepatocellular adenoma and focal nodular hyperplasia on gadoxetate disodium-enhanced MRI. *AJR Am J Roentgenol* 2011; 198: 115–123.
- [77] Gupta RT, Marin D, Boll DT, et al. Hepatic hemangiomas: difference in enhancement pattern on 3T MR imaging with gadobenate dimeglumine versus gadoxetate disodium. *Eur J Radiol* 2012; 81: 2457–2462.
- [78] Doo KW, Lee CH, Choi JW, Lee J, Kim KA, Park CM. “Pseudo washout” sign in high-flow hepatic hemangioma on gadoxetic acid contrast-enhanced MRI mimicking hypervascular tumor. *AJR Am J Roentgenol* 2009; 193: W490–W496.
- [79] Yoshimura N, Saito K, Saguchi T, et al. Distinguishing hepatic hemangiomas from metastatic tumors using T1 mapping on gadoxetic-acid-enhanced MRI. *Magn Reson Imaging* 2013; 31: 23–27.
- [80] Grazioli L, Kirchin M, Pirovano G, Spinazzi A. MultiHance in the dynamic phase of contrast enhancement: a pictorial assessment. *J Comput Assist Tomogr* 1999; 23(Suppl 1): S61–S64.
- [81] Motosugi U, Ichikawa T, Onohara K, Sou H, Sano K, Muhi A, Araki T. Distinguishing hepatic metastasis from hemangioma using gadoxetic acid-enhanced magnetic resonance imaging. *Invest Radiol* 2011; 46: 359–365.
- [82] Sun HY, Lee JM, Park HS, et al. Gadoxetic acid-enhanced MRI with MR cholangiography for the preoperative evaluation of bile duct cancer. *J Magn Reson Imaging* 2012; 38: 138–147. doi: 10.1002/jmri.23957.
- [83] Alegre Castellanos A, Molina Granados JF, Escribano Fernandez J, Gallardo Muñoz I, Triviño Tarradas F de A. Early phase detection of bile leak after hepatobiliary surgery: value of Gd-EOB-DTPA-enhanced MR cholangiography. *Abdom Imaging* 2012; 37: 795–802.
- [84] Kumazawa K, Edamoto Y, Yanase M, Nakayama T. Liver analysis using gadolinium-ethoxybenzyl-diethylenetriamine pentaacetic acid-enhanced magnetic resonance imaging: correlation with histological grading and quantitative liver evaluation prior to hepatectomy. *Hepatol Res* 2012; 42: 1081–1088.
- [85] Nojiri S, Kusakabe A, Fujiwara K, et al. Noninvasive evaluation of hepatic fibrosis in HCV-infected patients using EOB-MR imaging. *J Gastroenterol Hepatol* 2013; 28: 1032–1039. doi: 10.1111/jgh.12181.
- [86] Chen B-B, Hsu C-Y, Yu C-W, et al. Clinical and histologic implications of delayed hepatobiliary enhancement on magnetic resonance imaging with gadolinium ethoxybenzyl diethylenetriaminepentaacetic acid. *Invest Radiol* 2012; 47: 649–655.
- [87] Lau H, Man K, Fan ST, Yu WC, Lo CM, Wong J. Evaluation of preoperative hepatic function in patients with hepatocellular carcinoma undergoing hepatectomy. *Br J Surg* 1997; 84: 1255–1259.
- [88] Wibmer A, Prusa AM, Nolz R, Gruenberger T, Schindl M, Ba-Ssalamah A. Liver failure after major liver resection: risk assessment by using preoperative gadoxetic acid-enhanced 3-T MR imaging. *Radiology* 2013; doi:10.1148/radiol.13130210.
- [89] Rubbia-Brandt L, Audard V, Sartoretti P, et al. Severe hepatic sinusoidal obstruction associated with oxaliplatin-based chemotherapy in patients with metastatic colorectal cancer. *Ann Oncol* 2004; 15: 460–466.
- [90] Zdenkowski N, Chen S, van der Westhuizen A, Ackland S. Curative strategies for liver metastases from colorectal cancer: a review. *Oncologist* 2012; 17: 201–211.
- [91] Shin N-Y, Kim M-J, Lim JS, et al. Accuracy of gadoxetic acid-enhanced magnetic resonance imaging for the diagnosis of sinusoidal obstruction syndrome in patients with chemotherapy-treated colorectal liver metastases. *Eur Radiol* 2012; 22: 864–871.